

## Supporting Information

### Overcoming the Reticuloendothelial System Barrier to Drug Delivery with a “Don’t-Eat-Us” Strategy

*Yixuan Tang,<sup>†,#</sup> Xiaoyou Wang,<sup>†,#</sup> Jie Li,<sup>†</sup> Yu Nie,<sup>#</sup> Guojian Liao,<sup>†</sup> Yang Yu,<sup>†</sup> and  
Chong Li<sup>†\*</sup>*

<sup>†</sup> Key Laboratory of Luminescent and Real-Time Analytical Chemistry (Southwest University), Ministry of Education, College of Pharmaceutical Sciences, Southwest University, Chongqing 400715, P.R. China.

<sup>#</sup> National Engineering Research Center for Biomaterials, Sichuan University, Sichuan 610065, P.R. China.

\*Corresponding author: Chong Li, email: chongli2009@gmail.com.

# Table of Contents

Table of Contents .....	2
Abbreviations .....	4
Method: .....	5
Materials .....	5
Synthesis of Peptides .....	5
Preparation and Characterization of Liposomes .....	6
Preparation and Characterization of PLGA NP.....	6
Immunoprecipitation and Western Blotting .....	7
Cellular adhesion in RAW264.7.....	7
Cellular Uptake in RAW264.7 .....	7
<i>In Vitro</i> Blocking of SIRP $\alpha$ .....	8
Uptake Mechanism of liposomes in RAW264.7 .....	8
<i>In Vivo</i> and <i>Ex Vivo</i> Fluorescence Image .....	8
Pharmacokinetic Studies .....	8
FRET Assay .....	9
Isolation and immunofluorescence of KCs and LSECs .....	9
Phagocytosed Percentage of CL/DSL in KCs and LSECs .....	10
Cellular Uptake in bEnd.3.....	10
Fluorescence Images of Brain horizontal section .....	10
Pharmacodynamics Studies.....	11
Biocompatibility Study .....	11
Supporting Figures.....	13
Figure S1 .....	13
Figure S2.....	14
Figure S3.....	15
Figure S4.....	16
Figure S5.....	17
Figure S6.....	18
Figure S7.....	19
Figure S8.....	20
Figure S9.....	21
Figure S10.....	22
Figure S11 .....	23
Figure S12.....	24
Figure S13.....	25
Figure S14.....	26
Figure S15.....	27
Figure S16.....	28
Figure S17.....	29
Figure S18.....	30
Figure S19.....	31

Figure S20.....	32
Figure S21.....	33
Figure S22.....	34
Figure S23.....	35
Figure S24.....	36
Figure S25.....	37
Figure S26.....	38
Figure S27.....	39
Figure S28.....	40
Supporting Tables.....	41
Table S1.....	41
Table S2.....	42
Table S3.....	43
Reference .....	44

## **Abbreviations**

BBB: Blood brain barrier

CL: blank conventional liposomes

DS: D-Self peptide

DSL: D-Self peptide modified liposomes

FRET: Förster Resonance Energy Transfer

HCS: High Content Analysis System

HPTS: 1-hydroxypyrene-3,6,8-trisulfonic acid

KD: The equilibrium dissociation constant

NS: Natural self peptide

NSL: Natural self peptide modified liposome

PEG: Poly(ethylene glycol)

PLGA NP: poly (lactic-co-glycolic acid) nanoparticles

RES: reticuloendothelial system

SIRP $\alpha$ : signal regulatory protein alpha



## Method:

**Materials.** Egg Lecithin Phosphatidylcholine (LP) and Cholesterol (Cho) were provided by A.V.T. Pharmaceutical Ltd. (Shanghai, China). Egg Liss Rhod PE was purchased from Avanti Polar Lipid Inc. (Alabaster, AL, USA). PLGA (50:50, 0.67 dL/g) was provided by Lactel Absorbable Polymers (Birmingham, USA). DAPI, DiOC18(3) (DiO), DiIC18(3) (DiI), DiIC18(5) (DiD) and DiIC18(7) (DiR) were supplied by US Everbright Inc (Suzhou, China). Rabbit anti-F4/80, Rabbit anti-ZO-1, Rabbit anti-Claudin5, Alexa Fluor 488 labeled sheep anti-rabbit, HRP labeled sheep anti-rabbit and APC-labeled Donkey anti-rabbit were purchased from Bioss biotechnology co. LTD (Beijing, China). Phosphotyrosine antibody was supplied by BOSTER Biological Technology co.LTD (Wuhan, China). Rabbit anti-SIRP $\alpha$  was supplied by Proteintech Group, Inc (Wuhan, China). 8-Hydroxypyrene-1,3,6-trisulfonic acid (HPTS) was supplied by Ark Pharm, Inc. (Libertyville, USA). The other chemicals and reagents were of analytical grade.

**Cell lines and Animals.** RAW264.7 and bEnd.3 were provided by Cell bank of Chinese Academy of Sciences (Shanghai, China) and cultured in Dulbecco's modified Eagle's medium (DMEM) (BI, Israel) supplemented with 10% Fetal Bovine Serum (FBS) (Hyclone, USA), and detached for passage using 0.25% Trypsin/0.5mM EDTA (BI, Israel). Cells were kept in an incubation chamber at 37 °C and 5% CO<sub>2</sub> with a humidified atmosphere. *Cryptococcus neoformans* var. *grubii* (serotype A) strain H99 was purchased from American Type Culture Collection (ATCC, USA) and grown in nutrient-rich yeast extract-peptone-dextrose (YPD) medium at 30°C. The female Balb/c mice (4 weeks, 18-22 g) were purchased from Chongqing Academy of Chinese Materia Medica and raised in laboratory animal environment of SPF, housed on a 12-hour light/dark cycle at 22-24°C and 30-50% relative humidity. All animal experiments were conducted under guidelines of Ethical Review Committee of experimental animals at the Southwest University of China.

**Synthesis of Peptides.** Natural mouse "Self" peptide (NS) (palmitic acid-GNYTCEVTELSREGKTVIELK), D-mouse "Self" peptide (DS) (palmitic

acid-GK<sup>D</sup>L<sup>D</sup>E<sup>D</sup>I<sup>D</sup>V<sup>D</sup>T<sup>D</sup>K<sup>D</sup>GE<sup>D</sup>R<sup>D</sup>S<sup>D</sup>L<sup>D</sup>E<sup>D</sup>T<sup>D</sup>V<sup>D</sup>E<sup>D</sup>C<sup>D</sup>T<sup>D</sup>Y<sup>D</sup>N<sup>D</sup>G) and scrambled peptide (palmitic acid-GC<sup>D</sup>V<sup>D</sup>GS<sup>D</sup>T<sup>D</sup>E<sup>D</sup>E<sup>D</sup>E<sup>D</sup>V<sup>D</sup>Y<sup>D</sup>T<sup>D</sup>E<sup>D</sup>R<sup>D</sup>T<sup>D</sup>L<sup>D</sup>L<sup>D</sup>E<sup>D</sup>K<sup>D</sup>T<sup>D</sup>K<sup>D</sup>I<sup>D</sup>V<sup>D</sup>N<sup>D</sup>) were synthesized by means of solid phase peptide synthesis performed using Fmoc-protected amino acids and purified to homogeneity by reverse-phase high-performance liquid chromatography (HPLC), and their molecular weights were verified by electrospray ionization-mass spectrometry (ESI-MS).

**Preparation and Characterization of Liposomes.** Liposomes were prepared by thin-film evaporation method.<sup>1</sup> In brief, LP (dissolved in methanol) and Cho (dissolved in chloroform) were mixed at a molar ratio of 7:3. For liposomes modified with peptide, NS or DS were added at a molar ratio of 0.05% or as depicted in the related figures. The Egg Liss Rhod PE, DiI or DiR were added to weighed lipid film at a concentration of 40 µg Egg Liss Rhod PE per 8 mg LP, 10 µg DiI per 8 mg LP and 50 µg DiR per 8 mg LP, respectively. After vacuum drying overnight, the lipid film was hydrated with the distilled water at 37°C, and then ultrasonicated under an ice water bath and sequentially extruded through a polycarbonate membrane with pore sizes of 200 and 100 nm to prepare liposomes. Liposomes loaded with HPTS were also prepared by thin-film evaporation except that the mixed lipid film was hydrated in HPTS buffer (10 mM HPTS in PBS) before the formation of liposomes by extrusion. The size distributions and morphologies of various liposomes were determined by a dynamic light scattering method with a Zeta Sizer Nano Series (Nano ZS 90, Malvern, U.K.) and transmission electronic microscopy (TEM) (FEI Tecnai G20, USA), respectively. Every sample was measured in triplicate.

**Preparation and Characterization of PLGA NP.** The PLGA NP were prepared using nanoprecipitation.<sup>2, 3</sup> Briefly, 5 mg polymer was first dissolved in 1 mL acetone. For apamin (APA) modified PLGA NP, palmitic acid-apamin was added at 20 nmol peptide/mg PLGA (0.04mg/mg).<sup>4</sup> Then Coumarin 6, DiD, DiR and AmB were dissolved at a weight ratio of 0.1%, 0.1%, 0.2% and 5% to polymers respectively. The acetone solution was added dropwise to 10 ml of water under stirring. The mixture was then stirred in open air for 2 h and washed three times by ultrafiltration in Amicon tubes (MWCO 100kDa, Millipore). Then PLGA NP were concentrated and

resuspended with PBS to desired concentrations indicated by fluorescence intensity. For HPTS loaded PLGA NP, the aqueous phase was replaced by HPTS buffer (10 mM HPTS in PBS). The other steps were conducted as described above.

The size distribution of PLGA NP was detected by dynamic light scattering (Zetasizer Nano ZS90, Malvern). TEM and SEM were used for morphologic studies. TEM imaging was performed on LVEM5 (Delong instruments, USA) operating at 5 kV. SEM images were captured using JSM-7800F (JEOL, Japan) at an excitation voltage of 10 kV.

**Immunoprecipitation and Western Blotting.** RAW264.7 were seeded into 60mm petri dishes (Corning, USA) at a density of  $5 \times 10^4$  cells/mL and cultured for 24 h. Different liposomes were added into the dishes at a final concentration of 1 mg/mL and incubated for 1 h. After incubation, the cells were washed with cold PBS for 3 times and then lysed on ice in 400  $\mu$ L of lysis buffer supplied with 1% phosphatase inhibitors and 1% PMSF. For immunoprecipitation, whole lysate was mixed with anti-SIRP $\alpha$  antibody (Preteintech, China) conjugated to agarose A+G at 4°C overnight. Precipitated proteins were separated on 10% SDS-PAGE and transferred to PVDF membrane for Western Blotting, in which anti-phosphotyrosine and anti-SIRP $\alpha$  were applied followed by HRP-conjugated IgG as second antibodies.

**Cellular adhesion in RAW264.7.** Liposomes adhered to the cell membrane of RAW264.7 were prepared with methods as described previously, and the temperature was set at 4°C to prevent endocytosis.<sup>5</sup> In brief,  $2 \times 10^5$  RAW264.7 were seeded in 35 mm Petri dishes (Corning, USA) and cultured for 24 h. Then the dishes were transferred into 4°C for 30 min prior to the addition of the DiI loaded liposomes. After incubation with liposomes (1 mg/mL) for a given period of time, the cells were washed with cold PBS. The fluorescence intensities of the cells were measured by fluorescence-activated cell sorter (FACS) (BD Calibur, BD Biosciences, USA).

**Cellular Uptake in RAW264.7.** For uptake studies of liposomes, RAW264.7 were seeded in Cell Carrier-96 Ultra Microplates (PerkinElmer, USA) and cultured overnight. Then Egg Liss Rhod PE labeled liposomes were added to the wells at a final concentration of 1 mg/mL and incubated for different time intervals, among

which liposomes were replaced with fresh medium after incubated for 1 h. Then cells were washed twice with PBS, fixed with 4% paraformaldehyde (PFA) for 15min and cell membranes were stained with DiO (10 µg/mL) for 30 min at room temperature. Cell images were taken with a High Content Analysis System (HCS) (Operetta CLS, PerkinElmer, USA).

***In Vitro* Blocking of SIRPα.** To block SIRPα *in vitro*, we pre-incubated RAW264.7 with 5 µg/mL anti-mouse SIRPα antibody (APC labeled, Sino Biological) for 30 min, then DSL was added at a final concentration of 1 mg/mL and cells were cultured for another 1 h before flow cytometry analysis or Confocal imaging.

**Uptake Mechanism of liposomes in RAW264.7.** Cells were seeded into 24-well plate (Corning, USA) at a density of  $5 \times 10^4$  per well and cultured for 24 h. Then RAW264.7 cells were preincubated with various endocytosis inhibitors for 1 h, including chlorpromazine (40 µM) (inhibiting the endocytosis mediated by clathrin), colchicine (36 µM) (inhibiting the endocytosis related to microtubulin), monensin (14 µM) (blocking the acidification of the endosome), brefeldin A (40 µM) (inducing the disintegration of Golgi apparatus and inhibiting the transportation of phagocytosed substance to lysosome), Filipin (12.5 µM) (inhibiting the endocytosis mediated by caveolae).<sup>6-9</sup> The control groups were incubated with blank medium for the same period of time. Then 1 mg/mL DiI loaded CL or DSL were added into the wells and incubated for another 1 h. The mean cell fluorescence of 10000 cells was determined by BD FACS Calibur for each replica.

***In Vivo* and *Ex Vivo* Fluorescence Image.** For DiR loaded liposomes (CL/Dir and DSL/DiR), they were injected to mice by tail vein. Fluorescence and X-ray images were collected at predetermined time points by FX pro *in vivo* Imaging System (Carestream, USA). At the same time, mice treated with the same dose of liposomes were sacrificed for *ex vivo* imaging. For DiR loaded PLGA NP (PLGA NP/DiR), The collection of fluorescence images was conducted as described above.

**Pharmacokinetic Studies.** For DiD loaded PLGA NP, after pre-treatment with CL or DSL, DiD loaded PLGA NP were injected to mice at a dose of 20 µg DiD/kg mice weight by tail vein. After dosing, blood samples were collected at different time

points (15 min, 30 min, 1, 2, 4, 8, 12 and 24 h). Three animals were used for each group. Approximately 40  $\mu$ L of blood was collected from each mouse, and analyzed with a 384-well black plate (Greiner, Germany) in Infinite F200 pro multimode reader (Tecan, Switzerland) (excitation/emission: 595/665 nm). The DiD concentrations in blood were calculated with a standard curve covering the concentration range of 0.15-20 ng/mL.

For AmB loaded APA-PLGA NP (AmB-APA-PLGA NP), after pre-treatment with CL or DSL, AmB-APA-PLGA NP were injected to mice at a dose of 2 mg/kg mice weight by tail vein. After dosing, blood samples were collected from retro-orbital sites at different time points (30 min, 1, 2, 4, 8, 12 and 24 h). Prior to the analysis, AmB was extracted from the plasma by the addition of 0.8 mL of methanol to 0.2 mL of plasma. The mixture was vortexed for 5 min and centrifuged at 10,000 rpm for 10 min. The supernatant was collected and measured by HPLC.

The pharmacokinetic parameters were calculated using a two-compartmental model with PKsolver 2.0.<sup>10</sup>

**FRET Assay.** DiO (5  $\mu$ g per 8 mg LP, DiO: DiI = 1:3) were loaded into CL or DSL and then administrated to mice by vein injection. At predetermined time points of 30 min, 2 h and 24 h, mice were sacrificed and the livers were carefully excised and cut into 8- $\mu$ m-thick sections using a CM1950 freezing microtome (Leica, Germany). Sections were observed using HCS. FRET DiI signals were excited from 435–460 nm and collected from 515–580 nm. The DiO signal was obtained after excitation at 435–460 nm and collected from 470–515 nm. The ratio,  $I_{DiI}/(I_{DiO} + I_{DiI})$ , was calculated to quantify the FRET change, where  $I_{DiI}$  and  $I_{DiO}$  are the average intensities in the images.

**Isolation and immunofluorescence of KCs and LSECs.** KCs were isolated from Balb/c mice using collagenase by two-step perfusion method, separated by a single Percoll gradient centrifugal elutriation.<sup>33-34</sup> For Immunofluorescence staining of F4/80, cells were seeded in Cell Carrier-96 Ultra Microplates (PerkinElmer, USA) and cultured overnight. After fixed with 4%PFA and treated with 0.1% Triton X-100, cells were dyed with anti-F4/80(1:100 diluted) and followed with Alexa Fluor

488-conjugated secondary antibody. Observation was performed by HCS after the cells were dyed with DAPI (5 µg/mL) for 5 min.

For isolation of LSECs, the liver sinusoidal cells were firstly isolated by two-step perfusion method and concentrated by Percoll gradient centrifugal elutriation, and further purified with LSEC binding magnetic beads (Miltenyi).<sup>35</sup> For immunofluorescence staining of CD31, cells were seeded in Cell Carrier-96 Ultra Microplates (PerkinElmer, USA) and cultured overnight. After fixed with 4%PFA and treated with 0.1% Triton X-100, cells were dyed with anti-CD31 (1:100 diluted) and followed with Alexa Fluor 488-conjugated secondary antibody. For staining of SIRP $\alpha$ , fixed cells were dyed with APC labeled anti-SIRP $\alpha$  (5 µg/mL). Observation was performed by HCS after dyed with DAPI (5 µg/mL) for 5 min.

**Phagocytosed Percentage of CL/DSL in KCs and LSECs.** KCs and LSECs were seeded in 96-well plate and cultured overnight. Then HPTS loaded CL or DSL were added to the wells at a concentration of 1 mg/mL and incubated for 2 h, and then replaced by fresh medium and further incubated for 4 h. After that, cells were washed with PBS and analyzed as described in phagocytosis percentage assay.

**Cellular Uptake in bEnd.3.** bEnd.3 were seeded in Cell Carrier-96 Ultra Microplates (PerkinElmer, USA) and cultured overnight. Then different liposomes were added to the wells as depicted in the figures. After incubation for 2 h, cells were washed twice with pre-warmed PBS (37°C), and coumarin 6 loaded APA-PLGA NP (200 µg/mL) were added and further incubated for 2 h. Then cells were fixed with 4% PFA for 15min and cell nucleic acid was stained with DAPI (5 µg/mL) for 5 min at room temperature. Cell images were taken with HCS.

For quantitative analysis, briefly, cells were seeded into 12-well and cultured for 24 h. Then, different liposomes were added to each well and incubated for 2 h. After replacing the medium, coumarin 6-loaded APA-PLGA NP (200 µg/mL) were added and further incubated for 2 h. Cell fluorescence intensity was measured by FACS Calibur flow cytometry (BD Biosciences, USA).

**Fluorescence Images of Brain horizontal section.** At 2 h after injection of APA-PLGA NP, mice were anesthetized by intraperitoneal injection of pentobarbital

sodium (50 mg/kg) and then perfused with 40 ml ice-cold PBS followed by 80 ml of 4%PFA. Brains were removed from the skull and placed in 4%PFA over-night. Then the brains were washed with PBS and immersed in 30% sucrose solution over 2 d for dehydration. After that, brains were frozen in OCT (Sakura Tissue Tek), and sectioned at 8  $\mu$ m (CM1950, Leica). Then the sections were dyed with DAPI (5  $\mu$ g/mL) for 5 min, and images were captured by HCS and 5 $\times$  air objective. The whole brain images were reconstructed with Harmony<sup>®</sup> 4.8.

**Pharmacodynamics Studies.** BALB/c mice were anesthetized with isoflurane and then inoculated with the *C. neoformans* suspension (concentration  $5 \times 10^8$  cell/mL, dose 5  $\mu$ L/20 g) through foramen magnum 24 hours after an intraperitoneal injection of cyclophosphamide (2  $\mu$ g /20 g).<sup>11</sup>

After modeling, the infected mice were divided into 5 groups, i) Untreated, ii) PBS+AmB-PLGA NP, iii) CL (100mg/kg)+AmB-PLGA NP, iv) CL (400 mg/kg)+AmB-PLGA NP and v) DSL(100mg/kg) +AmB-PLGA NP, the dose of AmB is 2 mg/kg, The drug administration was performed at day 1, 3 and 5 postinfection through tail vein. The survival rates of the mice (n = 10/group) were observed for 30 days.

For brain fungal burden test, mice were sacrificed at day 7 and the brains were removed aseptically, weighed, and homogenized in sterile saline (1mL/g tissue). The number of CFU was determined by a plate dilution method in triplicate using yeast extract dextrose chloramphenicol agar, and colony counting was performed after 48 h of incubation at 30 °C.

For histopathological observation, On day 7 post-treatment, treated and untreated mice were anesthetized with isoflurane and sacrificed. The brains were carefully removed and collected for analysis. Samples were fixed in 4% formaldehyde and embedded in paraffin for sectioning. Sections were stained with Gomori methenamine silver (GMS) for histopathological examination under a light microscope.

**Biocompatibility Study.** Normal mice were divided into 5 groups, i) PBS, ii) PBS+AmB-APA-PLGA NP, iii) CL (100mg/kg)+AmB-APA-PLGA NP, iv) CL (400

mg/kg)+AmB-APA-PLGA NP and v) DSL(100mg/kg) +AmB-APA-PLGA NP, the dose of AmB is 2 mg/kg, The drug administration was performed at day 1, 3 and 5 through tail vein. The mice were sacrificed at day 7, Major organs (brains, hearts, livers, spleens, lungs, and kidneys) were fixed in 4% paraformaldehyde fixative solution and sections were obtained. Then, the sections were stained with hematoxylin and eosin (H&E), and observed using an optical microscope.



## Supporting Figures

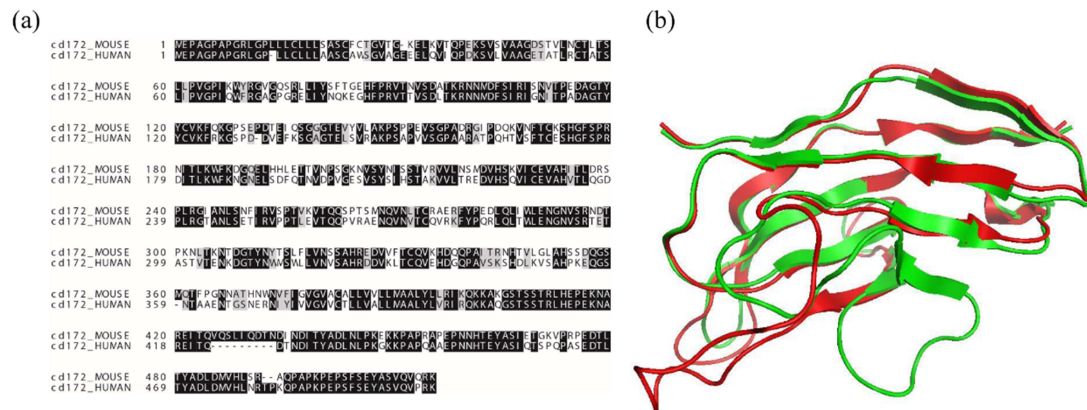


**Figure S1.** (a) Sequence alignment between mouse CD172a (SIRP $\alpha$ ) and human CD172a (SIRP $\alpha$ ), homologous sequence was shown as black background, functional concordance sequence was shown as grey background. (b) Homologous modeling of CD47. Human: green; mouse: red.



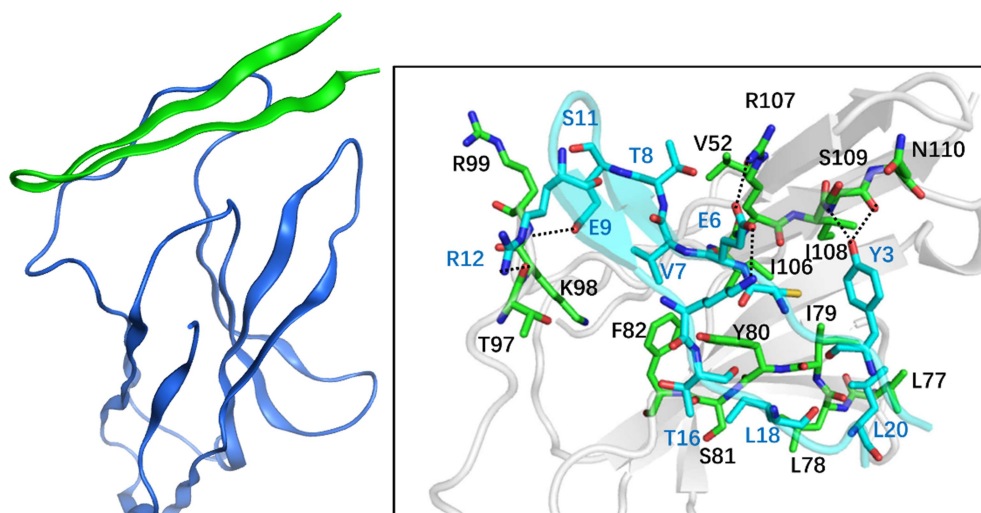


**Figure S3.** The interaction between natural mouse Self peptide (NS) and mouse SIRP $\alpha$ .

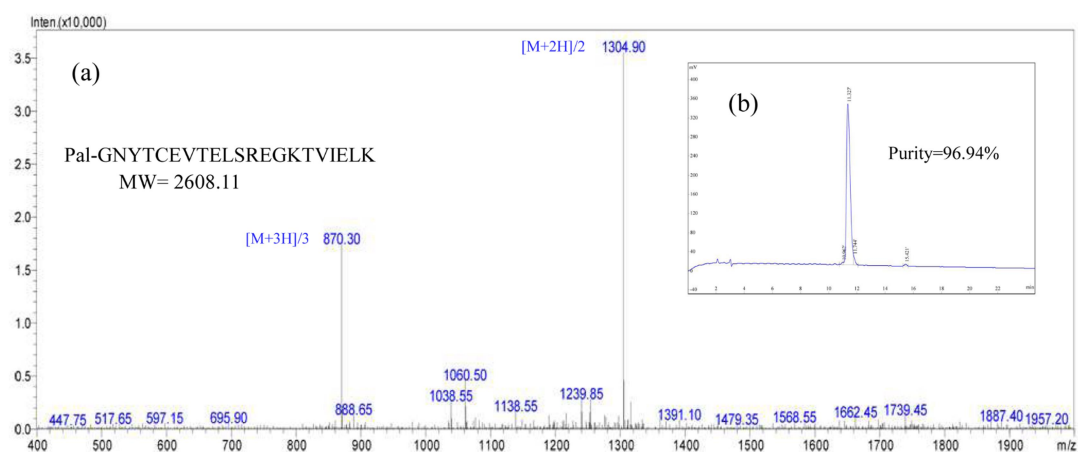


**Figure S4.** (a) The molecular weight of NS was certificated by ESI-MS and then (b) purity of peptide was affirmed by HPLC.

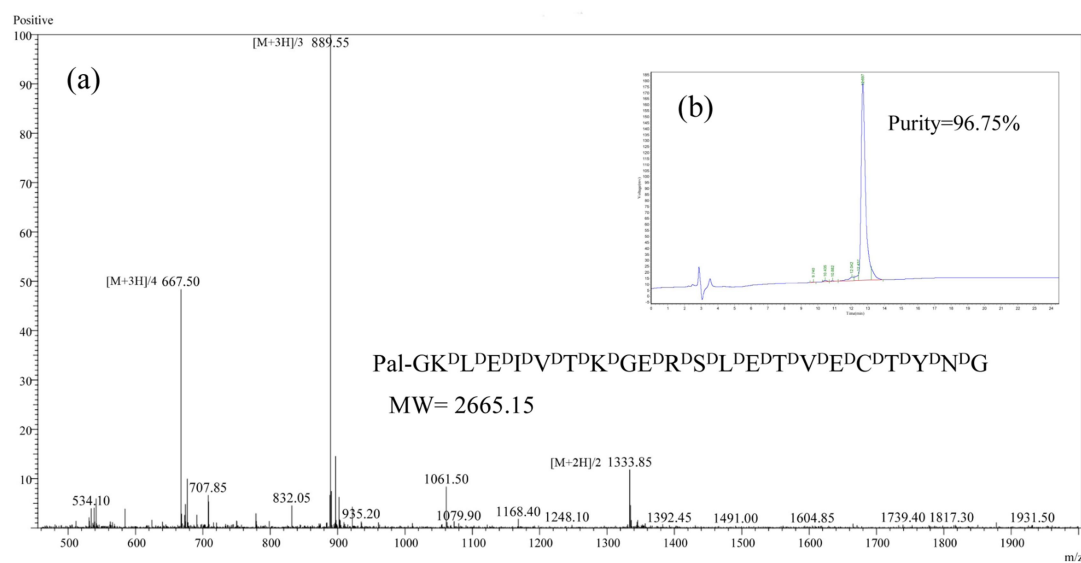


**Figure S5.** (a)The molecular weight of DS was certificated by ESI-MS and then (b) purity of peptide was affirmed by HPLC.

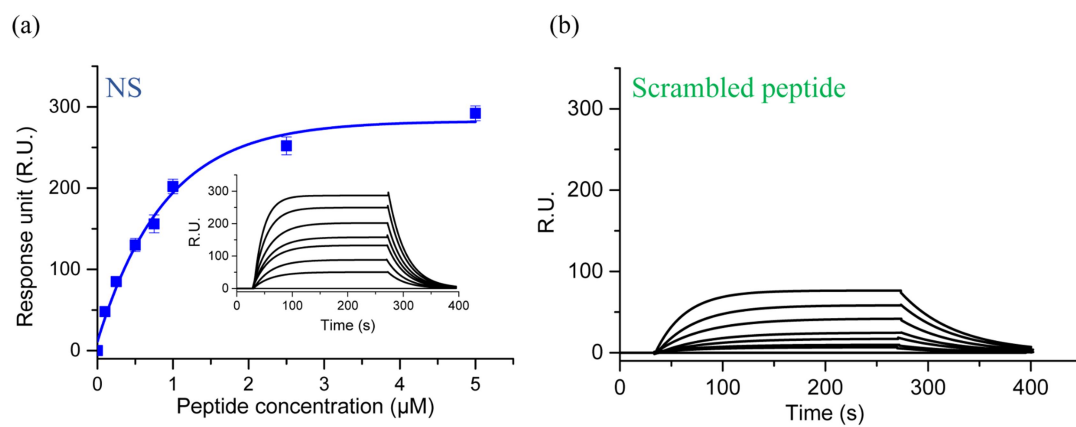


**Figure S6.** SPR response units between peptides and Mouse SIRP $\alpha$ .

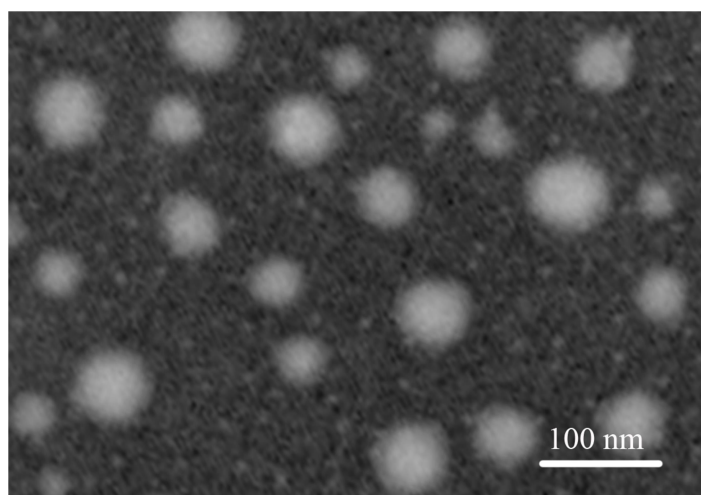


**Figure S7.** TEM image of DSL.

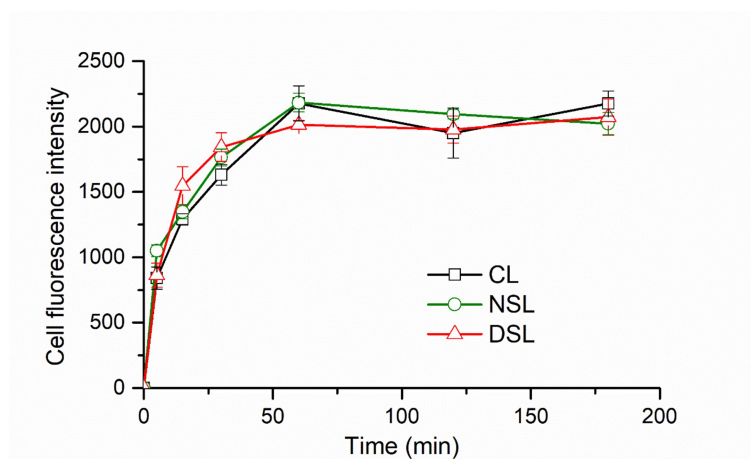


**Figure S8.** Adhering of different liposomes onto the cell membrane of RAW264.7, data are shown as mean $\pm$  SD (n=3).



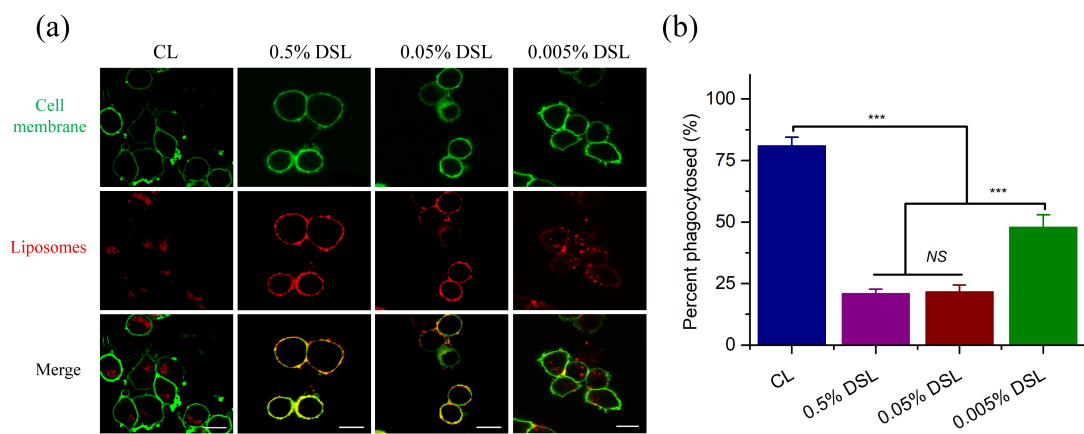


**Figure S9.** (a) Confocal images and (b) percent phagocytosed of RAW264.7 cells incubated with CL and DSL, DS were labeled on liposomes at a molar ratio of 0.5%, 0.05% and 0.005%, respectively. CL/DSL were removed after 1h of incubation, and then cells were cultured with fresh medium for another 5h. Scale bar= 10  $\mu$ m. \*\*\* $p$  < 0.001, NS represents non-significance, data are shown as means  $\pm$  SD (n = 3).

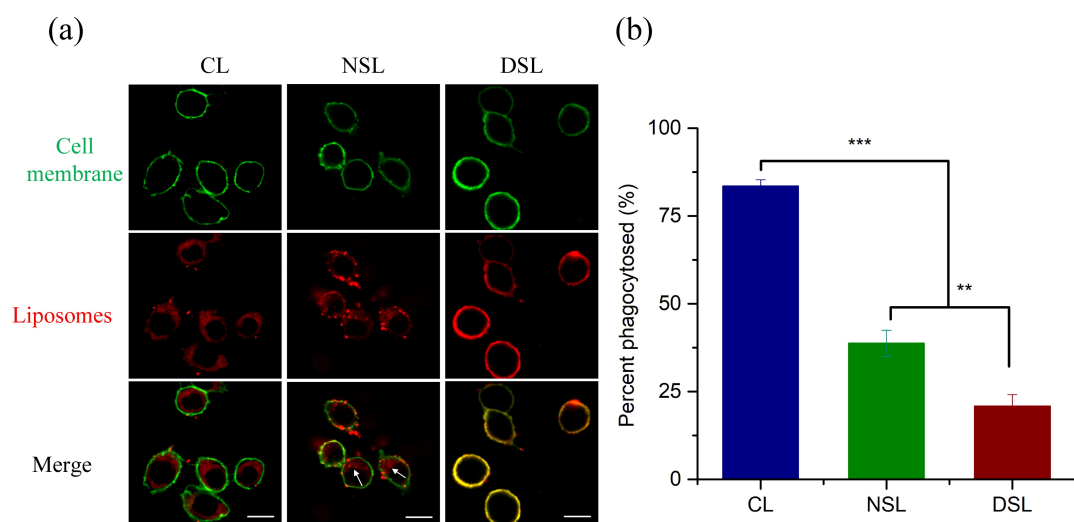


**Figure S10.** (a) Confocal images and (b) percent phagocytosed of CL, NSL and DSL in RAW264.7 cells. Liposomes were removed after 1h of incubation, and then cells were cultured with fresh medium for another 5h. Scale bar= 10  $\mu$ m. \*\*\* $p < 0.001$ , NS represents non-significance, data are shown as means  $\pm$  SD ( $n = 3$ ).

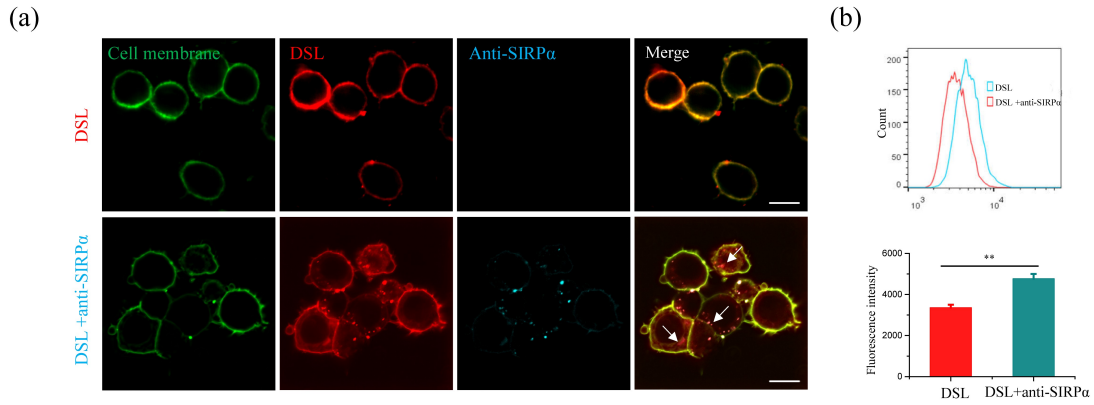


**Figure S11.** The effect of SIRP $\alpha$  on the uptake of DSL by RAW264.7. (a) Confocal images of RAW264.7 incubated with DSL (Liss Rhod PE EPC labeled) (red), cells were pre-incubated with APC labeled anti-SIRP $\alpha$  (Cyan) and cell membrane was labeled with DiO (green). The white arrows indicate the DSL phagocytosed by macrophage after SIRP $\alpha$  blocked with antibody. Scale bar= 10  $\mu$ m. (b) Cellular uptake of DiI-labeled DSL measured by FACS. RAW264.7 cells were pre-incubated with or without anti-SIRP $\alpha$ . \*\* $p < 0.01$ , Data are shown as mean  $\pm$  SD (n=3).

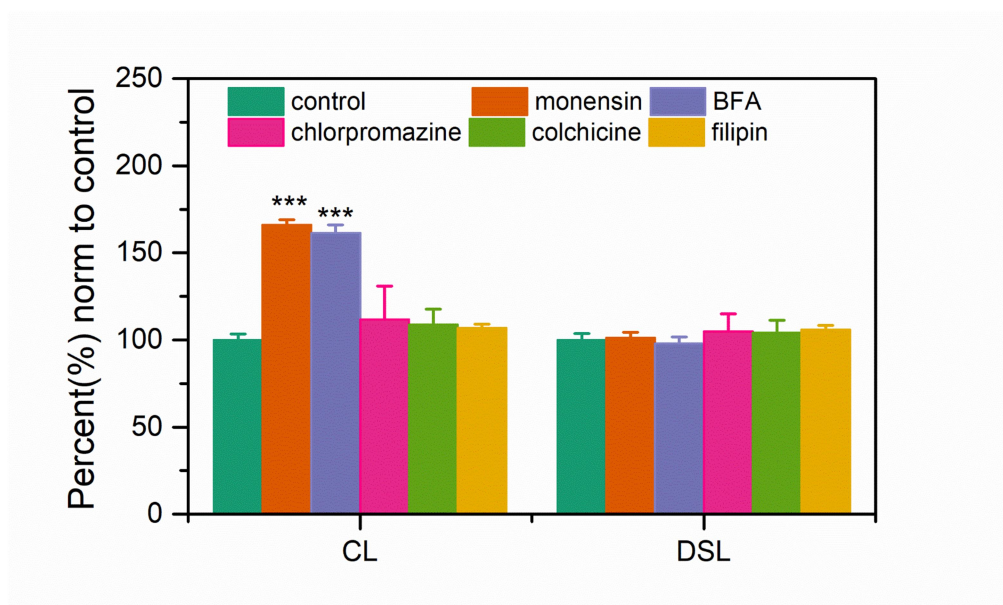


**Figure S12.** Cellular uptake mechanism of CL/DSL in RAW264.7. Five kinds of inhibitors were used in our experiments. Results were plotted percent normalized to corresponding non-treated groups, \*\*\* $p < 0.001$ . Data are shown as mean  $\pm$  SD (n=3). Interestingly, when macrophage was pretreated with BFA (inhibit the transportation of liposomes to lysosomes) or monensin (blocking the acidification of the endosome) which inhibit the cellular metabolism of liposomes, fluorescence intensity of CL treated macrophage was highly promoted whereas DSL treated cells showed no difference with control group, indicating the intracellular transportation of DSL in macrophages was not related to the clearance mediated by lysosomes.

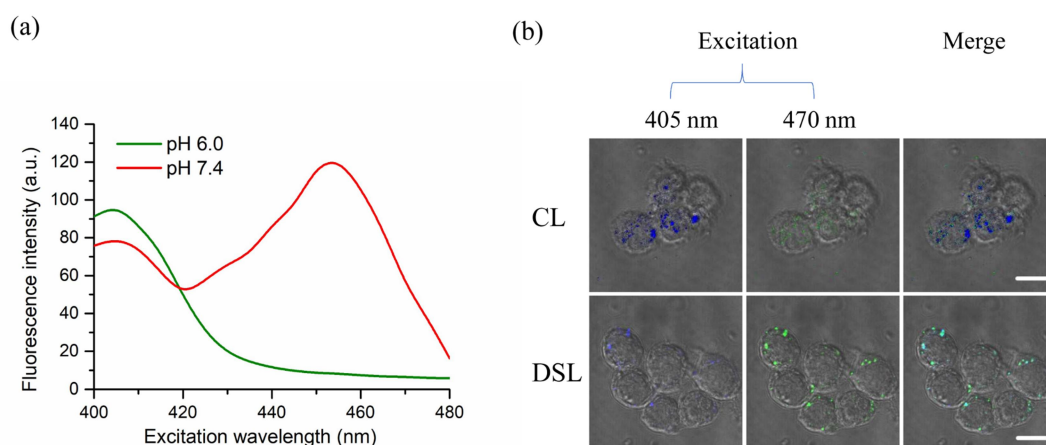


**Figure S13.** The pH-dependent properties of HPTS. (a) Excitation spectra of HPTS, the emission of HPTS was collected at 510nm and excitation were 400-480 nm. (b) Laser scanning microscopy images of RAW264.7. Cells were incubated with HPTS-loaded CL/DSL for 6 h. Fluorescence were observed by A1+R laser scanning confocal microscope (Nikon, Japan), scale bar=10μm.

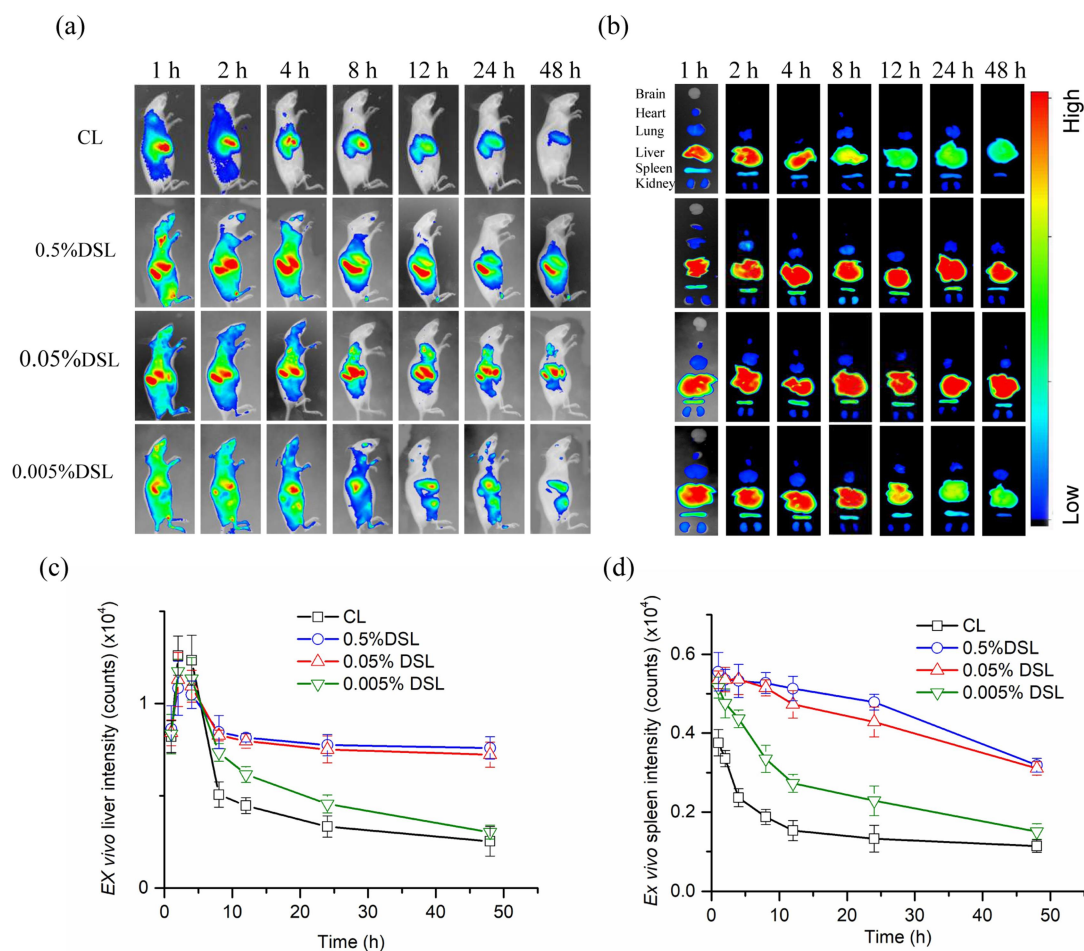


**Figure S14.** *In vivo* and *ex vivo* biodistribution of DiR loaded CL and DSL. DS were modified on liposomes at a molar ratio of 0.5%, 0.05% and 0.005%. Images of (a) whole-body and (b) main organs at different time points were collected respectively. (c) and (d) showed mean fluorescence intensity from the liver and spleen of mice treated with different liposomes. The results of *in vivo* and *ex vivo* distribution of CL and 0.05%DSL (abbreviated as DSL) was finally shown in the manuscript (Figure 3a). Fluorescence were quantified using Bruker MI SE 7.1. Data are shown as mean  $\pm$  SD (n=3).

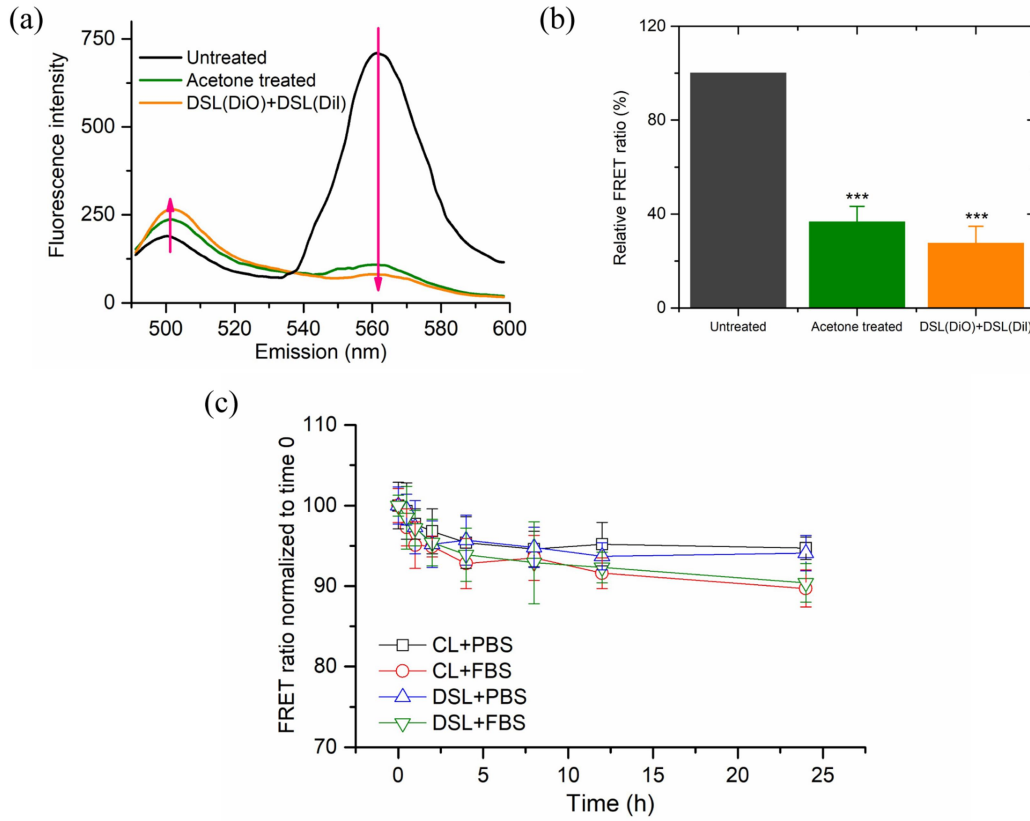


**Figure S15.** Establishing and stability of DiO/DiI FRET liposomes. (a) Change of FRET signal in the absence (Untreated) or presence of acetone, the mixture of DiO and DiI labeled DSL was served as control. Fluorescence signal was collected by microplate reader, excited at 450 nm and emission was collected from 480 nm to 600 nm. (b) Relative FRET ratio of integral and broken DSL, FRET ratio was calculated by Equation:  $I_{DiI} / (I_{DiO} + I_{DiI})$ , where  $I_{DiO}$  represents fluorescence intensity at 501 nm, and  $I_{DiI}$  represents fluorescence intensity at 565 nm, data are shown as the percent normalized to Untreated group (\* $p < 0.05$ , \*\* $p < 0.001$  and \*\*\* $p < 0.001$  as compared to Untreated) ( $n=3$ ). (c) The stability of FRET ratio, FRET ratio was measured for CL/DSL after incubation with PBS or whole FBS. Data are shown as mean  $\pm$  SD ( $n = 3$ ).

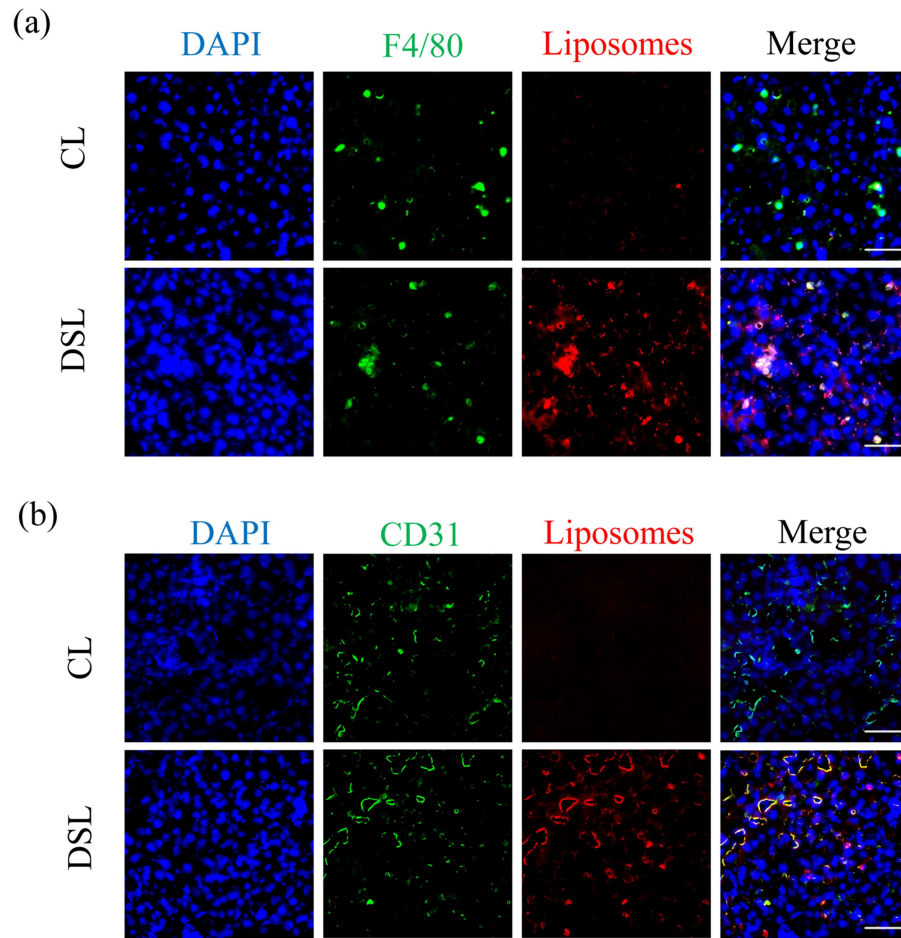


**Figure S16.** Fluorescence co-localization between liposomes and KCs/LSECs. Liver sections were prepared 24 h after liposomes were injected. (a) KCs were dyed with anti-F4/80 (green) and (b) LSECs were dyed with anti-CD31 (green), liposomes were labeled with Liss rhod PE EPC (red), scale bar=20  $\mu\text{m}$ .



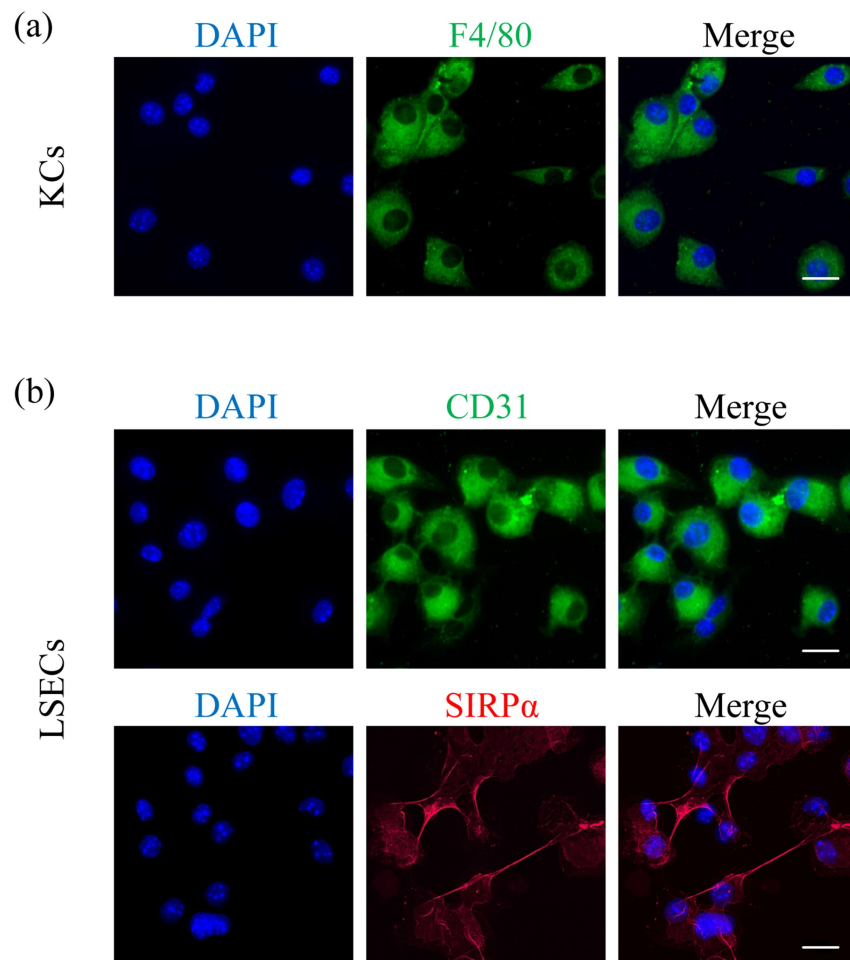


**Figure S17.** Immunofluorescence detection of KCs and LSECs. (a) KCs were stained with anti-F4/80, (b) LSECs were stained with anti-CD31 and anti-SIRP $\alpha$ . Scale bar= 10  $\mu$ m.

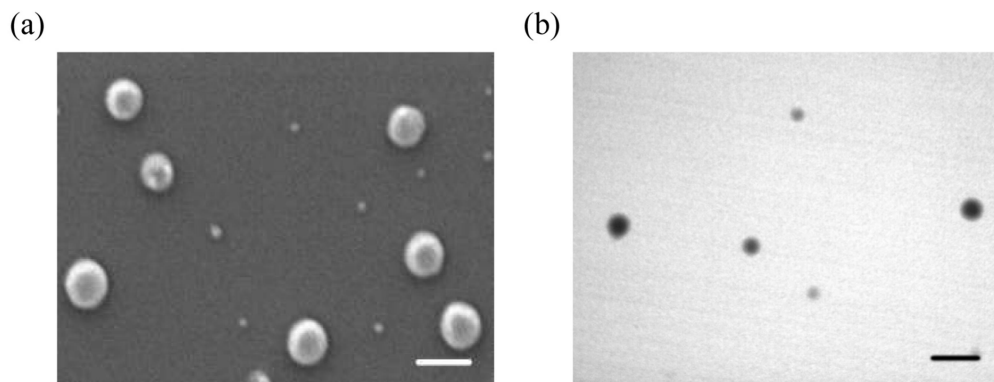


**Figure S18.** (a) SEM image of PLGA NP, scale bar= 100 nm. (b) TEM image of PLGA NP, scale bar= 200 nm.

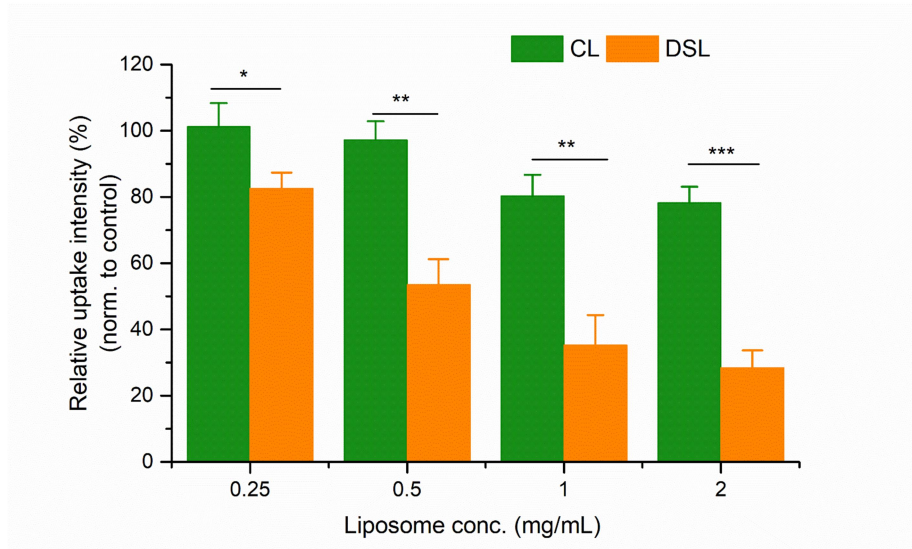


**Figure S19.** Uptake of PLGA NP by RAW264.7. Cells were pre-treated with different concentrations of CL/DSL for 1 h and washed with PBS, then DiD loaded PLGA NP (200  $\mu\text{g/mL}$ ) were added and further incubated for 6 h, the mean fluorescence of cells was measured by FACS. Data are shown as mean  $\pm$  SD(n=3) (\* $p < 0.05$ , \*\* $p < 0.001$  and \*\*\* $p < 0.001$ ).

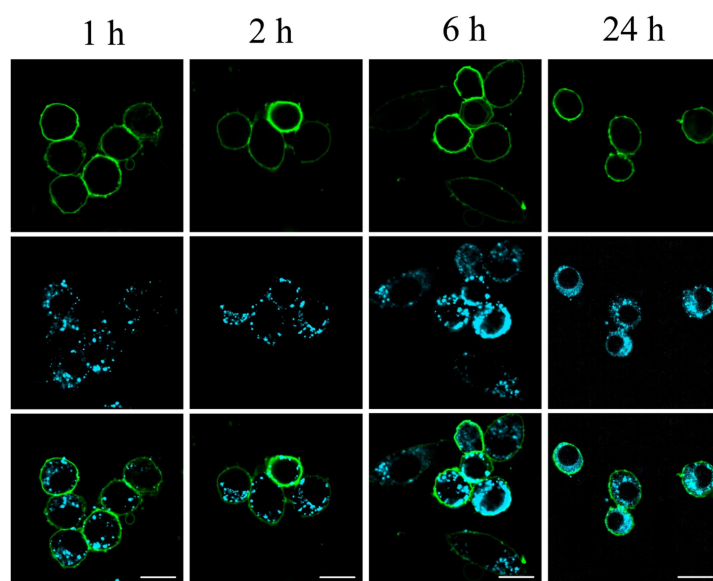


**Figure S20.** the uptake of PLGA NP by RAW264.7, cell membranes were labeled with DiO (green), PLGA were loaded with DiD (cyan). Scale bar=10 $\mu$ m.

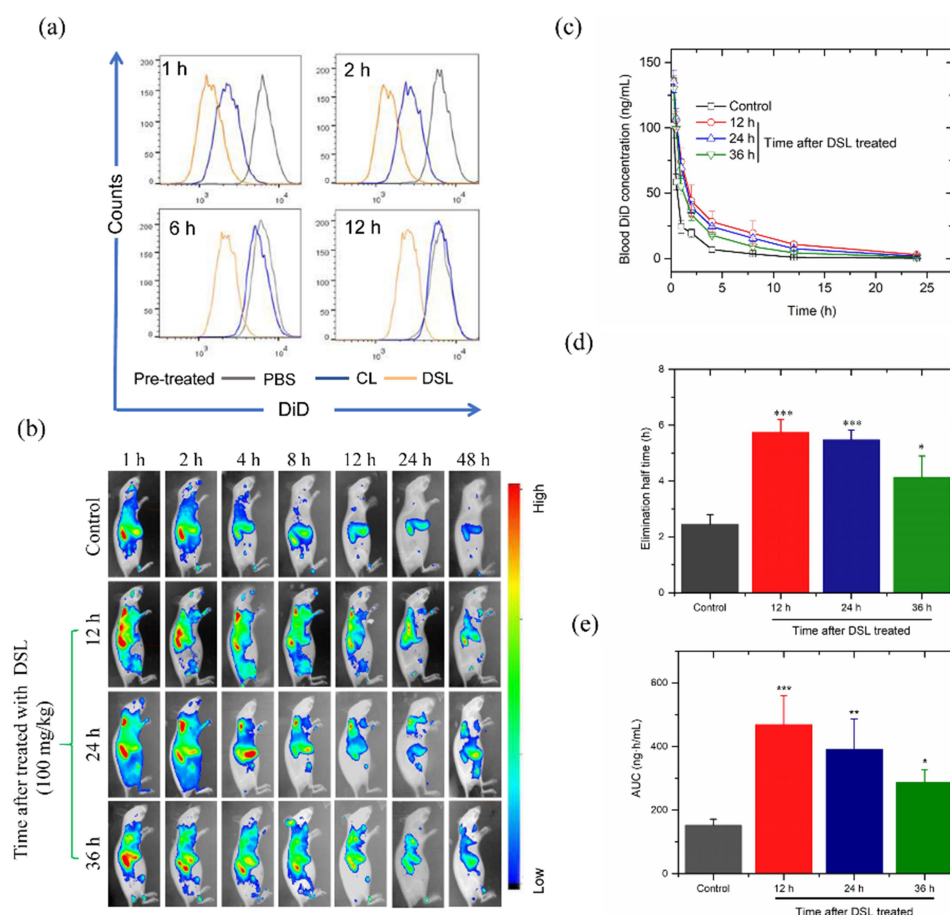


**Figure S21.** Mice treated with DSL showed a sustained tendency to delay the clearance of PLGA NP. (a) Uptake of PLGA NP by macrophage. Macrophage was pre-treated with CL (1 mg/mL) or DSL (1 mg/mL) for 1, 2, 6 and 12 h respectively, then incubated with PLGA NP for 2 h before FACS analysis. (b) *In vivo* real-time distribution of PLGA NP with different pre-treatments by living fluorescence imaging. Mice were pre-treated with DSL (100 mg/kg) for 12, 24 and 36 h, respectively. (c) Blood DiD concentration profile and related (d) elimination half time and (e) AUC of DiD after administration of PLGA NP (the administration dose of DiD was 20  $\mu$ g/kg). \* $p < 0.05$ , \*\* $p < 0.01$ , \*\*\* $p < 0.001$ , data are shown as mean  $\pm$ SD (n=3).

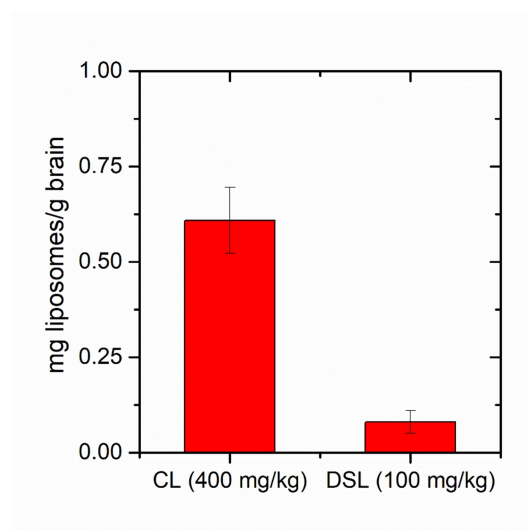


**Figure S22.** Biodistribution of liposomes in brain. CL and DSL were labeled with DiD at a ratio of 0.1% (wt/wt), then liposomes were injected to mice by tail vein. 2h after injection, mice were sacrificed, and blood and brains were collected respectively. The fluorescence intensities of DiD were measured by F200 pro multimode reader (Tecan, Switzerland) (excitation/emission: 595/665 nm), and the biodistribution of CL/DSL was calculated with the concentration of DiD correspondingly. Data are shown as mean $\pm$  SD (n=3).

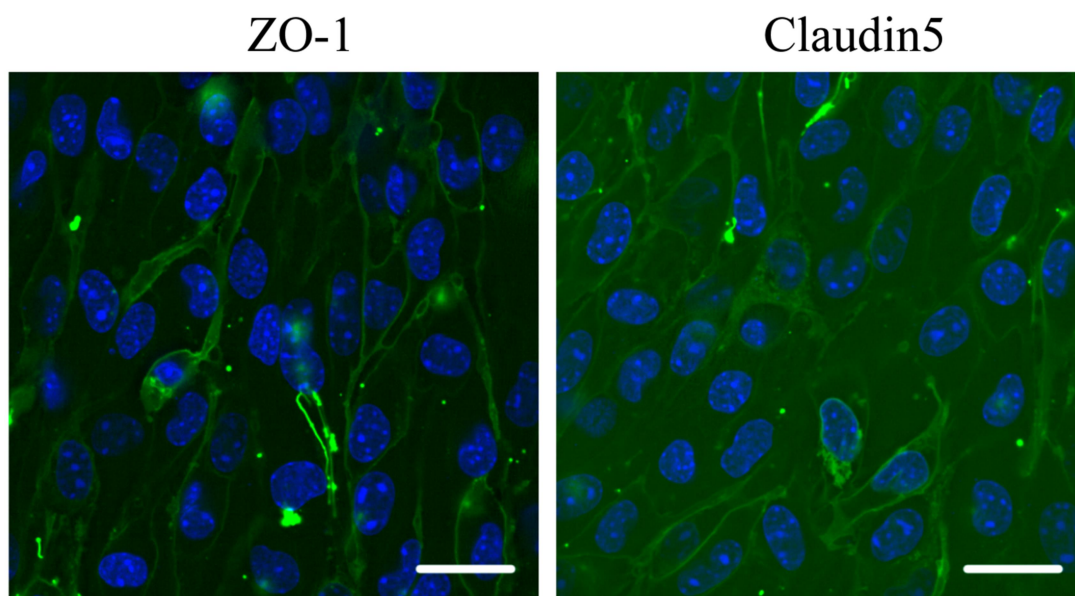


**Figure S23.** Subcellular localization of tight junction proteins in bEnd.3 cells. Cells were incubated in glass cover slips for 10 days. After fixed with 4%PFA and treated with 0.1% Triton X-100, cells were dyed with anti-ZO-1 (1:100 diluted) and anti-claudin 5 (1:100 diluted), respectively. And then followed with Alexa Fluor 488-conjugated secondary antibody. Observation was performed by HCS after dyed with DAPI (5  $\mu$ g/mL) for 5 min. Scale bar= 20  $\mu$ m.

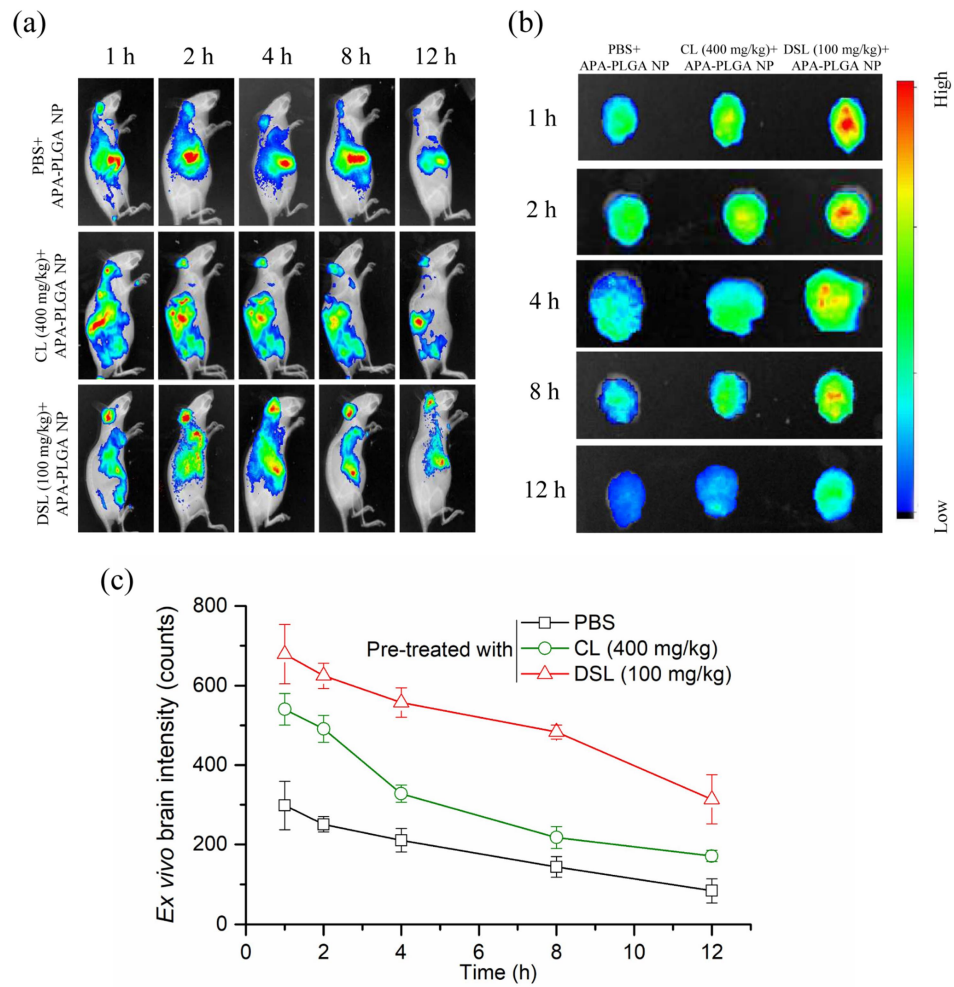
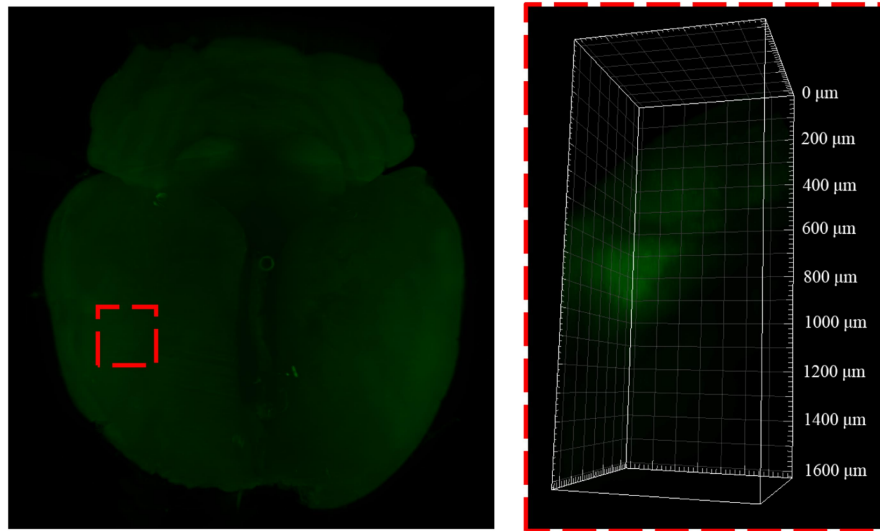


**Figure S24.** (a) *In vivo* and (b) *ex vivo* brain distribution of DiR loaded APA-PLGA NP. (c) showed mean fluorescence intensity from the brains. Data are shown as mean  $\pm$  SD (n=3).





PBS +APA-PLGA NP

**Figure S25.** Distribution of APA-PLGA (green) in whole brain, three-dimensional fluorescence images were observed by LSM.

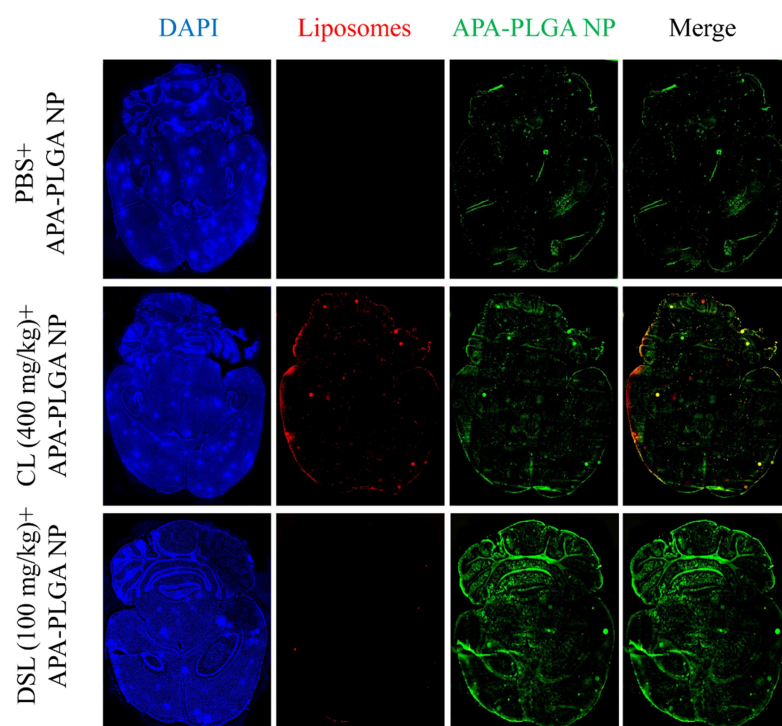


**Figure S26.** Horizontal brain fluorescence image of Coumarin 6-loaded PLGA NP.

(a)

	10 <sup>-1</sup>	10 <sup>-2</sup>	10 <sup>-3</sup>	10 <sup>-4</sup>
Control				
AmB-PLGA NP				
CL (100 mg/kg)+ AmB-PLGA NP				
CL (400 mg/kg)+ AmB-PLGA NP				
DSL (100 mg/kg)+ AmB-PLGA NP				

(b)

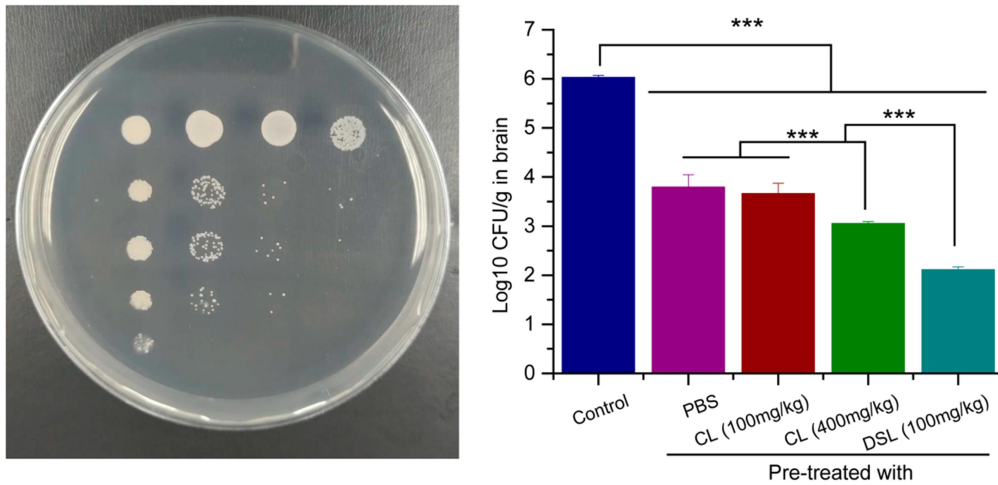


**Figure S27.** Tissue burden study of treatment groups showing their *in vivo* therapeutic effect against *Cryptococcus neoformans*. (a) Inoculation scheme of brain tissue homogenate from different treatment groups with serial dilution ratios (b) fungal growth of the inoculated homogenates from 7d treatment groups. \*\*\* $p < 0.001$ , data are shown as means  $\pm$  SD ( $n = 3$ ).

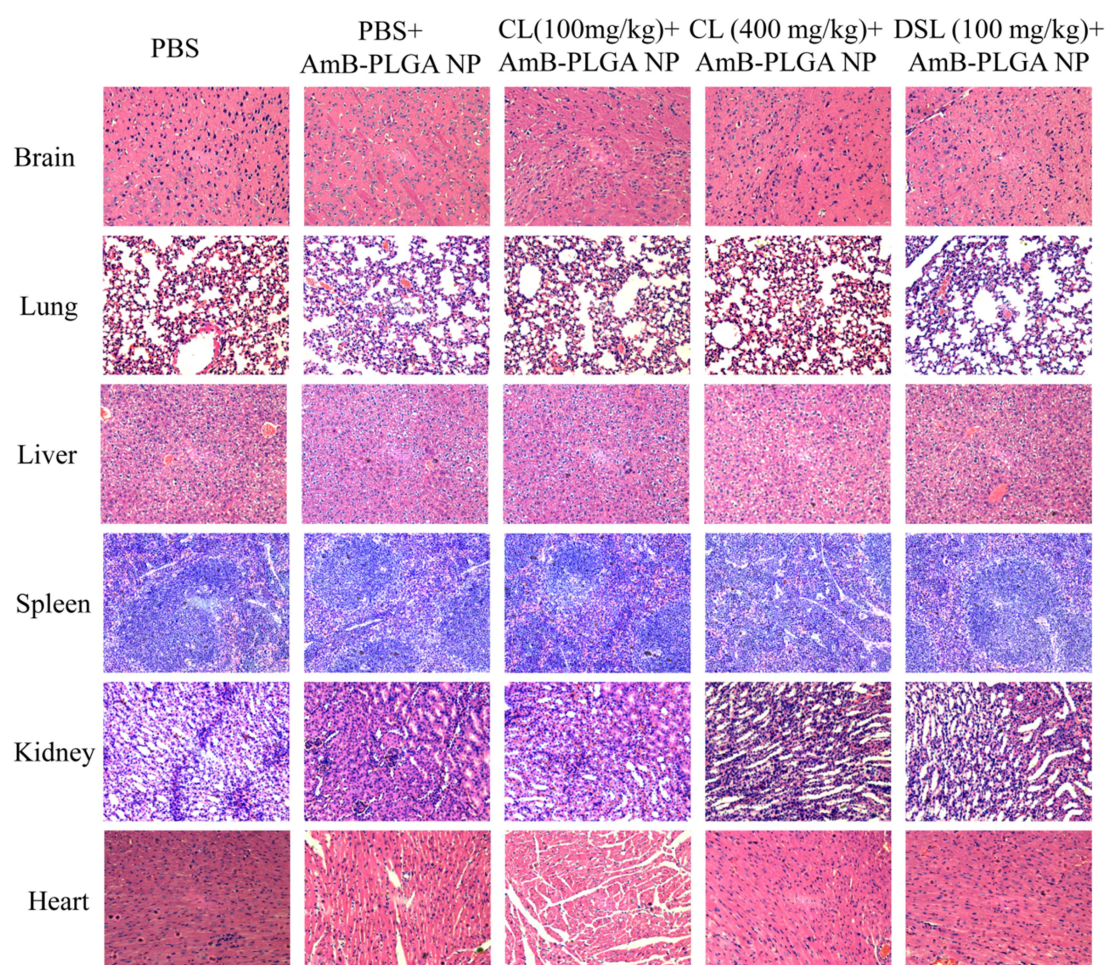


**Figure S28.** H&E staining of the main organs of the mice in different treatment groups.

## Supporting Tables

**Table S1.** Characterization of the liposomes and PLGA NP (n=3).

nanoparticles	Mean size(nm)	PDI	$\zeta$ (mV)
CL	89.2 $\pm$ 2.7	0.15 $\pm$ 0.01	-4.3 $\pm$ 0.1
0.05% NSL	85.5 $\pm$ 3.3	0.13 $\pm$ 0.02	-4.5 $\pm$ 0.2
0.5% DSL	87.2 $\pm$ 1.9	0.11 $\pm$ 0.02	-4.3 $\pm$ 0.2
0.05% DSL	85.6 $\pm$ 3.1	0.09 $\pm$ 0.01	-4.6 $\pm$ 0.5
0.005% DSL	86.6 $\pm$ 2.2	0.07 $\pm$ 0.02	-4.6 $\pm$ 0.3
PLGA NP	94.5 $\pm$ 4.3	0.13 $\pm$ 0.02	-24.6 $\pm$ 1.1
APA-PLGA NP	98.9 $\pm$ 5.1	0.18 $\pm$ 0.01	-25.8 $\pm$ 0.9

**Table S2.** Pharmacokinetic parameters obtained from mice treated with DiD-loaded PLGA NP by i.v. injection, mice were pre-injected with PBS or different liposomes for 2 h.

	Pre-treated with			
	PBS	CL (100 mg/kg)	CL (400 mg/kg)	DSL (100 mg/kg)
Elimination half-time (h)	2.06± 0.63	3.32± 0.82	3.77± 0.34 <sup>*</sup>	5.44± 0.40 <sup>***</sup>
AUC <sub>0-t</sub> (ng·h/mL)	174.13± 27.46	275.48± 38.98 <sup>**</sup>	599.20± 58.40 <sup>***</sup>	545.68± 38.49 <sup>***</sup>
AUC <sub>0-∞</sub> (ng·h/mL)	174.41± 29.31	294.15± 39.95 <sup>**</sup>	606.35± 53.82 <sup>***</sup>	568.95 ±54.42 <sup>***</sup>
MRT(h)	2.13± 0.47	3.38± 0.66	4.63± 0.46 <sup>**</sup>	7.21± 0.39 <sup>***</sup>

Data are shown as mean ±SD (n=3). \*p < 0.05, \*\*p < 0.01 and \*\*\*p < 0.001 as compared to PBS treated group.

**Table S3.** Pharmacokinetic parameters obtained from mice treated with DiD-loaded PLGA NP by i.v. injection, and mice were pre-injected with DSL (100 mg/kg) at 12h, 24h and 36h before PLGA NP was injected.

	Control	Time after DSL treated		
		12h	24h	36h
Elimination half-time (h)	2.26± 0.35	5.73± 0.47 <sup>***</sup>	5.47± 0.35 <sup>***</sup>	4.16± 0.76 <sup>*</sup>
AUC <sub>0-t</sub> (ng·h/mL)	152.19± 20.11	465.91± 92.50 <sup>**</sup>	398.48± 101.52 <sup>**</sup>	288.12± 41.42 <sup>*</sup>
AUC <sub>0-∞</sub> (ng·h/mL)	152.67± 20.25	492.97±102.15 <sup>**</sup>	413.82± 112.43 <sup>**</sup>	293.21± 40.22 <sup>*</sup>
MRT(h)	2.45± 0.31	7.25± 0.67 <sup>***</sup>	6.05± 0.58 <sup>***</sup>	4.18± 0.66 <sup>*</sup>

Data are shown as mean ±SD (n=3). \*p < 0.05, \*\*p < 0.01 and \*\*\*p < 0.001 compare to PBS treated group.

## References:

1. Wu, J.; Jiang, H.; Bi, Q.; Luo, Q.; Li, J.; Zhang, Y.; Chen, Z.; Li, C. Apamin-Mediated Actively Targeted Drug Delivery for Treatment of Spinal Cord Injury: More than Just a Concept. *Mol. Pharm.* **2014**, 11, 3210-3222.
2. Zhu, X.; Wu, J.; Shan, W.; Zhou, Z.; Liu, M.; Huang, Y. Sub-50 nm Nanoparticles with Biomimetic Surfaces to Sequentially Overcome the Mucosal Diffusion Barrier and the Epithelial Absorption Barrier. *Adv. Func. Mater.* **2016**, 26, 2728-2738.
3. Zhou, H.; Fan, Z.; Li, P. Y.; Deng, J.; Arhontoulis, D. C.; Li, C. Y.; Bowne, W. B.; Cheng, H. Dense and Dynamic Polyethylene Glycol Shells Cloak Nanoparticles From Uptake by Liver Endothelial Cells for Long Blood Circulation. *ACS Nano* **2018**, 12, 10130-10141.
4. Wang, H.; Zhao, Y.; Wang, H.; Gong, J.; He, H.; Shin, M. C.; Yang, V. C.; Huang, Y. Low-Molecular-Weight Protamine-Modified Plga Nanoparticles for Overcoming Drug-Resistant Breast Cancer. *J. Control. Release* **2014**, 192, 47-56.
5. Lesniak, A.; Salvati, A.; Santos-Martinez, M. J.; Radomski, M. W.; Dawson, K. A.; Åberg, C. Nanoparticle Adhesion to the Cell Membrane and its Effect On Nanoparticle Uptake Efficiency. *J. Am. Chem. Soc.* **2013**, 135, 1438-1444.
6. Rejman, J.; Bragonzi, A.; Conese, M. Role of Clathrin- And Caveolae-Mediated Endocytosis in Gene Transfer Mediated by Lipo- And Polyplexes. *Mol. Ther.* **2005**, 12, 468-474.
7. Hu, T.; Kao, C. Y.; Hudson, R. T.; Chen, A.; Draper, R. K. Inhibition of Secretion by 1,3-Cyclohexanebis(Methylamine), a Dibasic Compound that Interferes with Coatomer Function. *Mol. Biol. Cell* **1999**, 10, 921-933.
8. Mellman, I.; Fuchs, R.; Helenius, A. Acidification of the Endocytic and Exocytic Pathways. *Annu. Rev. Biochem.* **1986**, 55, 663-700.
9. Marschner, K.; Kollmann, K.; Schweizer, M.; Bräulke, T.; Pohl, S. A Key Enzyme in the Biogenesis of Lysosomes is a Protease that Regulates Cholesterol Metabolism. *Science* **2011**, 333, 87-90.
10. Zhang, Y.; Huo, M.; Zhou, J.; Xie, S. Pksolver: An Add-in Program for



Pharmacokinetic and Pharmacodynamic Data Analysis in Microsoft Excel. *Comput. Methods Programs Biomed.* **2010**, 99, 306-314.

11. Xu, N.; Gu, J.; Zhu, Y.; Wen, H.; Ren, Q.; Chen, J. Efficacy of Intravenous Amphotericin B-Polybutylcyanoacrylate Nanoparticles Against Cryptococcal Meningitis in Mice. *Int. J. Nanomedicine* **2011**, 6, 905-913.